

## Novel Imidazolyl Derivatives of 1,8-Acridinedione as Potential DNA-Intercalating Agents

A. Jamalian<sup>a</sup>, A. Shafiee<sup>a,b</sup>, B. Hemmateenejad<sup>c</sup>, M. Khoshneviszadeh<sup>a</sup>, R. Miri<sup>c,d</sup>, A. Madadkar-Sobhani<sup>e</sup>, S.Z. Bathaie<sup>f</sup> and A.A. Moosavi-Movahedi<sup>c,g,\*</sup>

<sup>a</sup>Department of Medicinal Chemistry, Faculty of Pharmacy, Tehran University of Medical Sciences, Tehran, Iran

<sup>b</sup>Pharmaceutical Sciences Research Center, Tehran University of Medical Sciences, Tehran, Iran

<sup>c</sup>Medicinal and Natural Product Chemistry Research Center, Shiraz University of Medical Sciences, Shiraz, Iran

<sup>d</sup>Department of Medicinal Chemistry, Faculty of Pharmacy, Shiraz University of Medical Sciences, Shiraz, Iran

<sup>e</sup>Institute of Biochemistry and Biophysics, University of Tehran, Tehran, Iran

<sup>f</sup>Department of Clinical Biochemistry, Faculty of Medical Sciences, Tarbiat Modares University, Tehran, Iran

<sup>g</sup>Center of Excellence in Biothermodynamics, University of Tehran, Tehran, Iran

(Received 20 February 2011, Accepted 26 May 2011)

The effect of twelve novel imidazolyl derivatives of 1,8-acridinedione (ligands) on calf thymus DNA was studied applying different biophysical techniques including UV-Vis spectrophotometry, CD spectropolarimetry and fluorimetric methods to gain deeper insights into the mechanism of interaction of the ligands with DNA. The binding parameters such as  $C_{50}$ ,  $K_{app}$ ,  $\Delta G^{\circ}_{(H_2O)}$  and  $m$ -value, followed by Scatchard analysis, indicate that among the tested ligands, four compounds; **12b**, **13b**, **12f** and **13f**, containing nitro and benzyl imidazole substituents, revealed uncompetitive intercalative mode of interaction with DNA. UV-Vis studies imply that the compounds bind cooperatively to DNA at the concentration range of 100-200  $\mu$ M. Based on biophysical data, QSAR analysis, and docking simulations, we propose that in cytotoxic 1,8-acridinediones, the imidazole moiety is essential for pharmacological activity and the introduction of more flexible and electron-withdrawing substituents on the imidazole ring serves to enhance their DNA intercalating ability.

**Keywords:** DNA-intercalation, Imidazolyl-1,8-acridinedione, Circular dichroism, Docking, QSAR

### INTRODUCTION

In spite of great advances in the treatment of cancer and the development of new approaches to interfere with cell cycle control, DNA still represents one of the most challenging bio-receptors for the development of small molecules [1]. Most compounds available interact with DNA non-covalently either through minor groove binding by a combination of

hydrophobic, electrostatic and hydrogen binding interactions, or *via* intercalative binding in which planar aromatic moiety slides between the DNA base pairs [1]. Understanding the mode of the interaction of small molecules with DNA is of significance in the rational design of more potent and selective anticancer agents and is being actively pursued. Although it is well established that DNA binding is not sufficient to confer cytotoxicity, interaction with DNA is often considered as a necessary criterion [1]. Accordingly, the synthesis of novel DNA interacting acridines such as 9-phenoxyacridines [2],

\*Corresponding author. E-mail: moosavi@ibb.ut.ac.ir

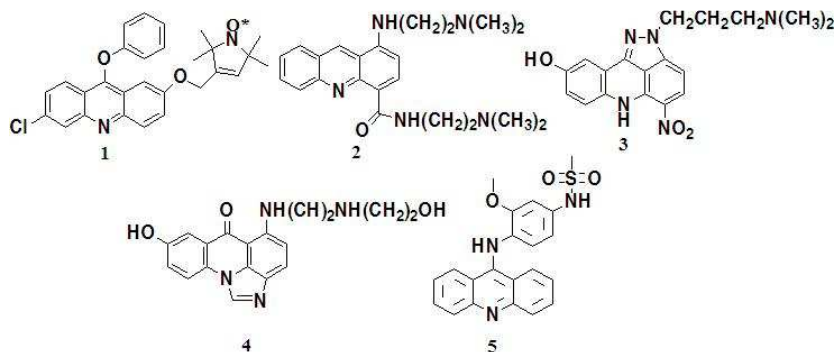


**Fig. 1.** Chemical structure of 9-phenoxyacridines (1), aminoalkyl-4-acridine carboximides (2), pyrazoloacridines (3), imidazoloacridinones (4), Amsacrine (9-aminoacridine) (5).

aminoalkyl-4-acridine carboximides [2], pyrazoloacridines [3] and imidazoloacridinones [4,5] is being explored. Amsacrine (a 9-aminoacridine) and Ledakrin (a nitro-acridine) are used clinically and several derivatives such as the 4-carboxamidoacridine (DACA) are currently undergoing clinical trials [6]. The structures of compounds mentioned are shown in Fig. 1.

Among different acridine derivatives, 1,8-acridinedione is a known scaffold with a wide spectrum of biological properties such as anti-malarial activity [7,8], potassium channel opening effect [9-11], DNA interaction and anti-tumor effects [12,13]. The diverse physicochemical properties of this agent such as oxido-reduction and Nicotinamide Adenine Dinucleotide Phosphate (NADPH) are well established [14].

We were thus strongly encouraged to obtain some deeper insights into the mechanism of the interaction of the synthesized imidazolyl derivatives of 1,8-acridinedione with calf thymus DNA and to attain a wider appreciation of any ligand-DNA interaction and characterization.

## EXPERIMENTAL

### Materials and Methods

Calf thymus (CT) DNA was obtained from Sigma-Aldrich. All DNA solutions used were prepared in 5 mM Tris buffer (pH = 7.4) at 4 °C, giving a UV absorbance ratio ( $A_{260}/A_{280}$ ) of 1.83 indicating that DNA was sufficiently free of protein. Concentration of DNA stock solution (1.18 mg ml<sup>-1</sup>) in nucleotide phosphate (NP) was determined by UV absorbance

at 260 nm and the extinction coefficients of CT-DNA solutions ( $\epsilon_{260}$ ) were taken as 6600 M<sup>-1</sup> cm<sup>-1</sup> at 260 nm, expressed in micromolar base ( $\mu$ Mb) [15]. The ethidium bromide (EtBr) was obtained from Sigma Aldrich in analytical grade, and its 1 mM stock solution was prepared in Tris-HCl buffer freshly before each experiment.

### Synthesis

A series of novel imidazolyl derivatives of 1,8-acridinediones were synthesized in our laboratories and the structure of the compounds (ligands) under experiment and their physical and spectral properties have been reported previously [16].

### UV-Visible Spectrophotometry

All the spectrophotometric measurements were carried out using a Rayleigh, UV-2100 UV-Vis, recording double-beams spectrophotometer. Absorption of aqueous solution of the compounds was proportional to their concentrations in the range of  $2 \times 10^{-6}$  to  $2 \times 10^{-3}$  M. The absorption changes of fixed amount of DNA upon titration with increasing ligand concentration with ratios of 0.08, 0.24, 0.56, 1.36, 2.16, 2.96, 3.76, 6.16, 8.16 and 12.16 were used to determine  $\Delta G^{\circ}_{(H_2O)}$  of denaturation according to Pace method [17-20]. In this experiment the sample cell was filled with DNA solution and the reference cell was filled with Tris-HCl buffer only. After 3 min, the absorption was recorded at 260 nm for DNA. The addition of ligand to both cells continued until no further

changes were observed. These absorption readings of DNA solutions were plotted separately versus different concentrations of the ligands. From these plots the concentration of each ligand at the midpoint of transition was deduced and the concentration of the ligand in the transition region was calculated (we picked 50, 100 and 150  $\mu\text{M}$  concentration of each ligand for further experiments).

The fraction of denatured DNA ( $F_d$ ) was calculated using the following equation:



$$F_d = (A_n - A_{\text{obs}})/(A_n - A_d) \quad (2)$$

where  $F_d$  is the fraction of denatured DNA,  $A_{\text{obs}}$  is the observed absorption of DNA at each concentration of the ligand (50, 100 and 150  $\mu\text{M}$ ), and  $A_n$  and  $A_d$  are the absorption values for the native and denatured states, respectively. Therefore, the difference between the free energy of the native and the modified forms of DNA ( $\Delta G^\circ$ ) were calculated using the following equation [17-20]:

$$\Delta G^\circ = -RT \ln[F_d/(1-F_d)] = -RT \ln[(A_n - A_{\text{obs}})/(A_{\text{obs}} - A_d)] \quad (3)$$

where  $R$  is the gas constant ( $1.986 \text{ cal K}^{-1} \text{ mol}^{-1}$ ) and  $T$  is the absolute temperature (298.15 K). The plot of the values of  $\Delta G^\circ$  against the denaturant concentration revealed a linear behavior shown in the following equation [17-20]:

$$\Delta G^\circ = \Delta G^\circ_{(\text{H}_2\text{O})} - m [D] \quad (4)$$

where  $\Delta G^\circ_{(\text{H}_2\text{O})}$  is the conformational stability of DNA in the absence of the ligand (the value of  $\Delta G^\circ$  at the zero concentration of the ligand),  $m$  is a measure of the ligand ability to denature DNA, and  $[D]$  is the denaturant concentration. The procedure is reported for DNA in the presence of the compounds separately. The calculated  $\Delta G^\circ_{(\text{H}_2\text{O})}$  and  $m$  values are presented in Table 1.

### Fluorimetric Measurements

Fluorescence emission spectra were obtained by Cary Eclipse, Varian model, (Australia), (quartz cuvette, 1 cm)

operated in energy mode. Both slit widths employed were 5 nm for the excitation and emission beam. The spectra were recorded at  $10 \text{ nm min}^{-1}$  scanning speed without filter. The emission spectrum of EtBr was studied at its maximum quantum yield at 471 nm. All of the compounds exhibited rather strong fluorescence allowing measurements at as high concentrations as 100 nM. Fluorescent emission of all the studied compounds was proportional to their concentration in the range of  $1 \times 10^{-5}$  to  $1 \times 10^{-3}$  M. The fluorimetric study of the interaction of EtBr with DNA in the absence and presence of the ligands was carried out applying the method reported by Strothkamp & Strothkamp [21,22] at 25 °C. For EtBr displacement assay excitation was set at 471 nm, and fluorescence emission was monitored in the range 550-700 nm [21,22]. Since the fluorescence intensity of DNA-ethidium complex can be altered due to the binding of ligands to the complex, the effect of each ligand was studied in this respect. Experiments were performed with an EtBr on DNA molar ratio of 1.26 and a drug concentration range of 4-200  $\mu\text{M}$  in a Tris-HCl buffer, pH = 7.4.  $C_{50}$  values (concentration of the ligand required to reduce the initial EtBr fluorescence by 50%) for EtBr displacement were calculated using a fitting function and the apparent equilibrium binding constants ( $K_{\text{app}}$ ) were calculated using Eq. (5) [21,22]:

$$K_{\text{app}} = \left( \frac{[\text{DNA}]/[\text{EB}]}{C_{50}} \right) \times K_{\text{EtBr}} \quad \text{with } K_{\text{EtBr}} = 10^7 \text{ M}^{-1} \quad (5)$$

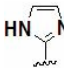
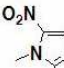
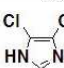
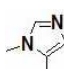
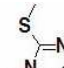
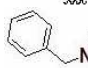
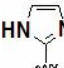
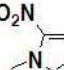
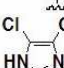
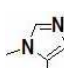
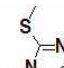
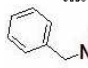
Results are shown in Table 2.

### Scatchard Analysis

The Scatchard analysis was carried out according to the method previously described in the literature [23-26]. Three sets of nine samples containing constant concentration of DNA and different concentrations of EtBr (0, 2, 4, 6, 8, 10, 14, 18 and 20  $\mu\text{M}$ ) were prepared. The solutions were kept at room temperature for the inhibition time (about 30 min) and were then treated with different concentrations of each ligand (50, 100 and 150  $\mu\text{M}$ ). The emission intensities were recorded at 605 nm.

The emission intensity of free EtBr-DNA ( $I_0$ ) for nine EtBr solutions (0, 2, 4, 6, 8, 10, 14, 18 and 20  $\mu\text{M}$ ) in buffer and emission intensity of DNA-ligand-EtBr ( $I_1$ ) were recorded.

**Table 1.** The Calculated Parameters of DNA Stability in the Absence and Presence of the Effective Concentration of Each Ligand

Ligand	R	$\Delta G^{\circ}_{(H_2O)}$ (kcal mol <sup>-1</sup> )	$m$ (kcal mol <sup>-1</sup> $\mu$ M <sup>-1</sup> )	R <sup>2</sup>
No ligand	-	18.779	0.0156	0.999
12a		6.0627	0.0794	0.9881
13a		9.784	0.0512	0.8801
12b		8.2443	0.0328	0.9947
13b		8.4541	0.0418	0.9342
12c		8.196	0.0629	0.9555
13c		12.269	0.0432	0.8139
12d		13.813	0.0524	0.9615
13d		10.004	0.0488	0.9701
12e		18.732	0.1705	0.9975
13e		9.1563	0.0944	0.9999
12f		10.76	0.0642	0.9280
13f		8.399	0.1366	0.9268

**Table 2.** Apparent Binding Constants ( $K_{app}$ ) and  $C_{50}$  Values of the Ligands in 5 mM Tris-Buffer and pH = 7.4

Compound	$C_{50}(\mu\text{M})^a$	$K_{app}\times 10^6{}^b$
<b>12a</b>	178.1	0.071
<b>13a</b>	470.92	0.027
<b>12b</b>	91.64	0.137
<b>13b</b>	88.49	0.142
<b>12c</b>	219.4	0.033
<b>13c</b>	192.61	0.065
<b>12d</b>	215.17	0.059
<b>13d</b>	326.60	0.039
<b>12e</b>	223.39	0.057
<b>13e</b>	204.50	0.062
<b>12f</b>	122.80	0.103
<b>13f</b>	108.30	0.116

<sup>a</sup>Concentration of the compound required to reduce the initial EtBr fluorescence by 50%. <sup>b</sup>The apparent binding constant.

Applying the data, the number of EtBr molecules bound to DNA ( $C_b$ ) was worked out using:

$$C_b = I_t - I_0 / (V - I)K \quad (6)$$

where  $K$  is the slope of the  $I_0$  against the added EtBr concentration ( $C_0$ ).  $V$  is the ratio of emission intensities of bound EtBr to free EtBr, which has been reported 50 in average in most articles. These intensities should be determined under precisely the same conditions considering solvent, temperature, concentration, and excitation wavelength. In our experiment, the slope of the  $C_{EtBr}$  curve against  $C_b$  was 51.8 ( $r^2 = 0.933$ ).

The value of  $r$  can be calculated with the determination of  $C_b$ :

$$r = C_b / [\text{DNA}] \quad (7)$$

where  $r$  is the ratio of bound EtBr to the total DNA concentration. Through plotting  $r/C_f$  against  $r$ , the Scatchard plot was obtained ( $C_f$  is the free concentration of EtBr from  $C_f = C_0 - C_b$ ). The Scatchard plots of the selected ligands are shown in Fig. 4.

### Circular Dichroism Spectropolarimetry (CD)

The CD spectra were obtained via a J-810 Jasco spectropolarimeter at 25 °C controlled by a PTC-423S/L Peltier type cell changer (Jasco). A quartz cell of 10 mm path length was used to obtain spectra from 200 to 320 nm with a resolution of 0.1 nm. The CD measurements were performed in a 5 mM Tris-HCl buffer, pH = 7.4 for DNA to ligand concentrations of 0.04, 0.1, 0.2, 0.75 and 1.5 in each case. Data are reported in  $\theta$  (ellipticity) (mdeg) or molar ellipticity  $[\theta] \times 10^{-3}$  (degree  $\text{cm}^{-1}/\text{dmol}$ ), based on the average weight of nucleotide (AWN), which is equal to 330 for DNA (for oligonucleotide is obtained according to their sequence) [27-29].

### Docking Protocol

The three-dimensional structure of the molecules were constructed using HyperChem (HyperCube Inc., Gainesville, FL). Docking simulations were carried out using AutoDock [30] version 3.0.5 and crystal structure of Adriamycin in the complex with DNA hexamer (PDB ID: 1D12) [31] as described before [32].

### QSAR Analysis

The chemical structure of the molecules was constructed

using HyperChem package (Version 7, Hypercube Inc.). The Z-matrices of the structures were provided by the software and then transferred to the Gaussian 98 program [33]. Complete geometry optimization was obtained taking the most extended conformations as the starting geometries and employing semi-empirical molecular orbital calculations (AM1). HyperChem, Gaussian 98 and Dragon packages (R. Todeschini, Milano Chemometrics and QSAR Group <http://www.disat.unimib.it/vhm/>) were used for the calculation of molecular descriptors [34].

The highest occupied molecular orbital (HOMO) and the lowest unoccupied molecular orbital (LUMO) energies, the most positive charge (MPC), the least negative charge (LNC), the most negative charge (MNC), and the molecular dipole moment (MDP) were calculated by Gaussian98. Some chemical parameters including molar volume (V), molecular surface area (SA), hydrophobicity (logP), hydration energy (HE) and molecular polarizability (MP) were calculated using HyperChem software. Different topological indices such as first Zagreb index by valence vertex degrees (ZMV1) and ramification index, geometrical indices such as 3D Petijean shape index (PJI3) and constitutional indices were calculated using Dragon software.

The MLR analysis was performed by the SPSS software using the stepwise selection and elimination procedure for the variables [35]. For each set of descriptors, the best multi-linear regression equations were obtained, utilizing correlation coefficient ( $R^2$ ), standard error of regression (SE), correlation coefficient for cross-validation significance ( $Q^2$ ), root mean square error (RMS) and significant level (p-value). As co-linearity degrades the performances of the MLR-based QSAR equation, first correlation analysis was performed to detect the co-linear descriptors [36]. To do so, the correlation of descriptors with each other and with the biological and biophysical data was examined and from among the co-linear descriptors one of which represented the highest correlation more actively was retained and the rest were omitted.

## RESULT AND DISCUSSION

### DNA Binding Studies

**UV-Vis absorption titration experiments.** To avoid repetition, the results of compounds **12d** and **13d** as the

prototype of the less cytotoxic ligands and compounds **12b**, **13b**, **12f** and **13f** as the four more active compounds are demonstrated in the figures. On the other hand, the UV spectra of most of the compounds under experiment, exhibited slight hypochromic changes upon titration with CT-DNA compounds **12b**, **13b**, **12f** and **13f** revealed relatively pronounced hypochromic effect and induced bathochromic shift (3-5 nm) in the absorption maxima at 260 nm (Fig. 2). Upon intercalating of the base pairs of DNA, the  $\pi^*$  orbital of the intercalated ligand is coupled with the  $\pi$  orbital of the DNA base pairs, thus decreasing the  $\pi \rightarrow \pi^*$  transition energy and resulting in bathochromism.

On the other hand, the coupling  $\pi$  orbital was partially filled with electrons, thus decreasing the transition probabilities and concomitantly resulting in the hypochromism. This hypochromism effect seems to strongly depend on the substituents on the imidazole ring. As with the four compounds, **12b**, **13b**, **12f** and **13f**, in which the C<sub>5</sub>-hydrogen and the N<sub>1</sub>-nitrogen are replaced by a nitro and a benzyl group, respectively, the changes of UV-Vis spectra are comparatively more prominent implying the involvement of stronger  $\pi$ - $\pi$  stacking interactions with DNA duplex.

Absorbance plots against concentration revealed a curvilinear concave downwards suggesting a cooperative binding and the plateau phase in absorptions above 200  $\mu$ M (Fig. 2), suggesting 50-200  $\mu$ M transition concentration region of the ligands.

**DNA stability estimation.** Using the DNA denaturation plots and the Pace method [20], the values of  $F_d$  or unfolding equilibrium constant (Eq. 2.), and  $\Delta G^\circ$ , the unfolding free energy (Eq. 3.) of DNA at room temperature in the presence of the ligands were calculated. A straight line was obtained when the values of  $\Delta G^\circ$  were plotted versus the concentration of each ligand in the transition region. The  $m$  value, the slope of these plots (a measure of the ligand ability to denature DNA) and the intercept,  $\Delta G^\circ_{(H_2O)}$ , (conformational stability of DNA in the absence of the ligand) [17-20,37,38] are summarized in Table 1. The results clearly reveal that increasing the concentration of compounds **12b**, **13b**, **12f**, **13f**, **12d** and **13d** decreases the stability of DNA.

$\Delta G^\circ_{(H_2O)}$  is free energy in the absence of the ligand and is the best criterion for estimation of the stability of the biomacromolecule. The decrease in  $\Delta G^\circ_{(H_2O)}$  is indicative of

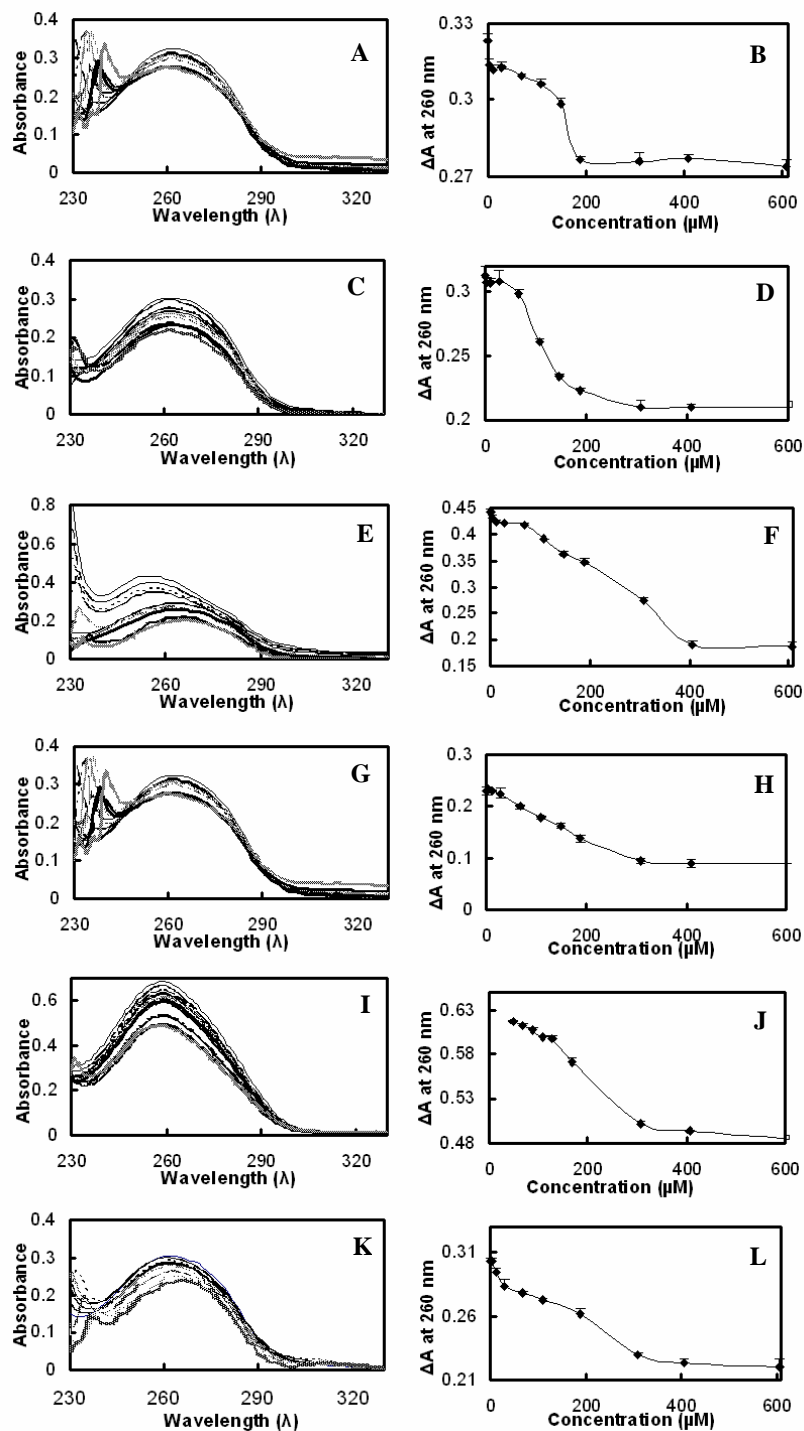


**Fig. 2.** UV spectra of (A) **12b**, (C) **13b**, (E) **12f**, (G) **13f**, (I) **12d**, and (K) **13d**. The adjacent curves show the plot of UV changes against ligand concentration in each case (B) **12b**, (D) **13b**, (F) **12f**, (H) **13f**, (J) **12d**, (L) **13d**.

diminishing of DNA stability due to interaction with ligands.  $\Delta G^{\circ}_{(H_2O)}$  values calculated for ligands **12b**, **13b** (8.2 and 8.4 kcal mol<sup>-1</sup>, respectively) and **12f** and **13f** (10.7 and 8.4 kcal mol<sup>-1</sup>, respectively) are clearly lower than the values calculated in “no ligand” condition and in comparison to other ligands such as **12d** and **13c** (13.81 and 12.27 kcal mol<sup>-1</sup>, respectively), showing that they strongly decrease the DNA stability, induce conformational changes, and make them more susceptible to denaturation, in comparison to other ligands (see Table 1). The value of *m* is a measure of the dependence of  $\Delta G^{\circ}$  on the denaturant concentration, so the higher *m*-value is linked to the stronger effect of the ligand interaction with DNA. The *m*-values of the said ligands did not show a significant difference in comparison to the other tested compounds, except for **13f**, whose *m*-value is 14 times higher than **12a**.

### Intercalation Studies Using Fluorimetric Methods

**EtBr displacement assay.** The ability of the ligands to displace the DNA intercalator EtBr from CT-DNA was probed by monitoring the relative fluorescence of the EtBr-DNA adduct after treating the DNA with varying concentrations of the ligands [21,22,39]. Strong fluorescence of the studied compounds in aqueous media allowed titration to be done exclusively at variable DNA to ligand concentration ratios. As is clearly shown in Fig. 3, the addition of increasing concentrations of each ligand to the DNA-EtBr complex, quenched the fluorescence emission of the complex. This could be attributed to the ability of the compounds to compete with EtBr in sliding between DNA base pairs.  $C_{50}$  values (concentration of the ligand required to reduce the initial EtBr fluorescence by 50%) for EtBr displacement were calculated using a fitting function, and the apparent equilibrium binding constants ( $K_{app}$ ) were calculated [21,22,39]. Among all the tested ligands, compounds **12b**, **13b** ( $C_{50}$  value of 91.6 and 88.5  $\mu$ M, respectively) and **12f** and **13f** (with  $C_{50}$  value of 122.8 and 108.3  $\mu$ M, respectively), showed a significantly more competitive binding potency in comparison to others, such as **13a** (470.9  $\mu$ M) or **12e** (223.4  $\mu$ M) (Table 2). A knowledge of equilibrium binding constant of the tested compounds facilitates an understanding of the affinity of a ligand towards DNA.

Compounds **12b**, **13b**, **12f** and **13f** clearly reveal the

highest binding constants alongside others. Ligand **13b** showed a binding constant of almost 5 times higher than **13a**. This obviously indicates that the mentioned compounds are capable of interaction with  $\pi$ -stacking of the DNA base-pairs (intercalation).

**Scatchard binding mode analysis.** The Scatchard analysis of the fluorescence quenching experiments provides information about the mechanism of ligand binding. As it can clearly be seen through Scatchard graphs (Fig. 4), in all ligands, except **12d** and **13d**, the cumulative binding constants remain constant and the number of the binding sites per nucleotide does not show any significant changes. This sort of interaction is described as un-competitive mode of interaction of small molecules. However, in the case of **12b**, **13b**, **12f** and **13f**, as the added concentration is increased, the cumulative binding constant decreases and the number of binding sites per nucleotide change in different magnitudes, which characteristically describe the non-competitive intercalation interaction [23-26,39].

**Circular dichroism spectropolarimetry.** Compounds **13d**, **12b** and **13f** as the representatives of each group were subjected to more detailed investigation through CD. In order to get a deeper insight into the changes of polynucleotide properties induced by small molecule bindings, CD spectropolarimetry was chosen as a highly sensitive method to detect the effect of intercalators on the base stacking and helicity of the double-strand DNA. The chiral compounds under experiment did not exhibit any band in the CD spectra region under investigation. The CT-DNA in the B-conformation shows two conservative CD bands in the UV region, a positive band at around 273 nm (due to base stacking) and a negative band at 242 nm (due to polynucleotide helicity) [17].

As indicated in Fig. 5E, very small changes were observed in the spectra of DNA-ligand **13d** which implies interaction with minor conformational changes in the DNA structure, whereas Figs. 5A (**12b**) and 5C (**13f**) are indicative of much more changes of the DNA conformation revealing a significant distortion in both  $\pi$ -stacking of the DNA base pairs and the helicity of the polynucleotide. While the changes do not fit to the intercalative binding mode, a non-competitive intercalative interaction accompanied by clear conformational changes in DNA structure can be deduced. As it is observed in



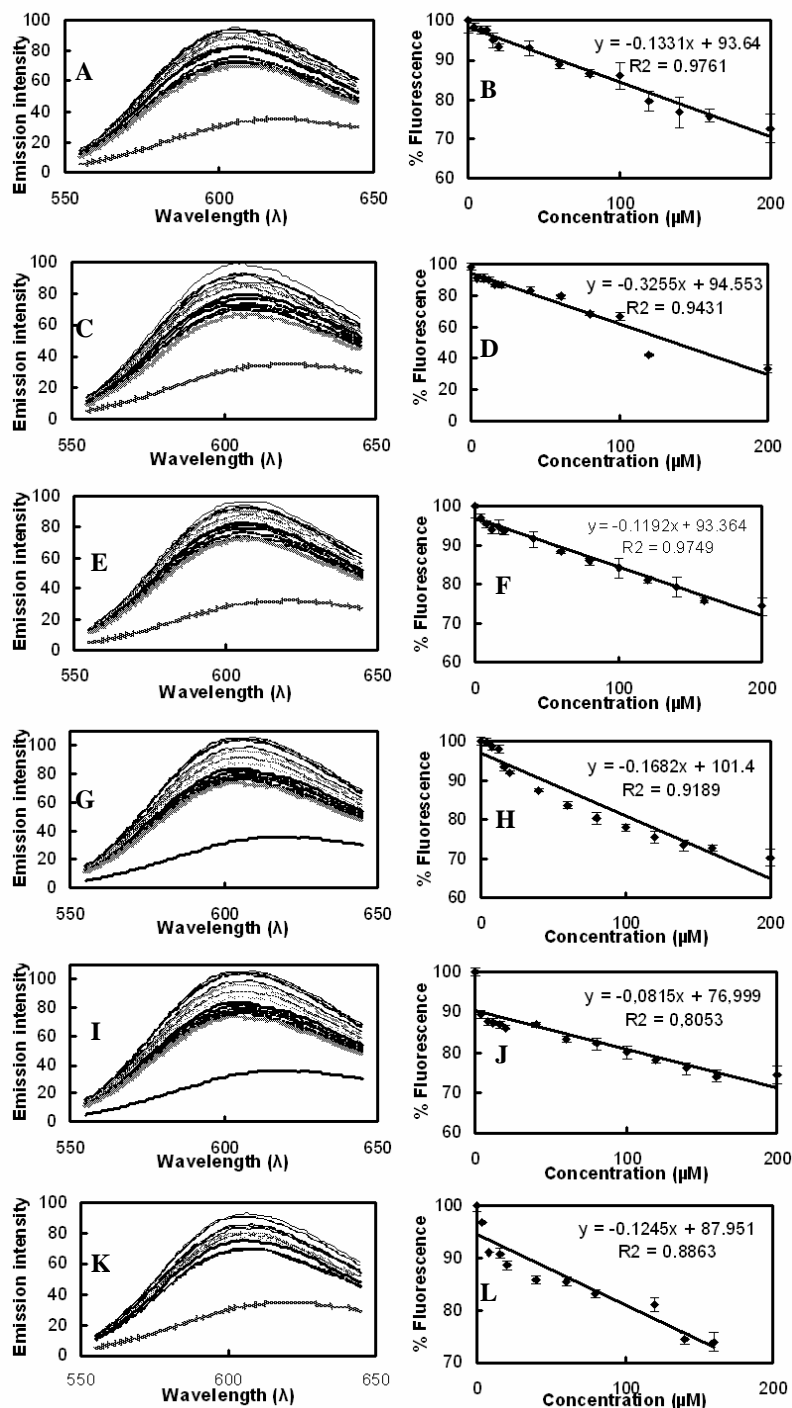


**Fig. 3.** Emission spectra of EtBr alone, and EtBr bound to CT-DNA in the absence and presence of different concentration of (A) **12b**, (C) **13b**, (E) **12f**, (G) **13f**, (I) **12d**, and (K) **13d**, in Tris-HCl buffer (5 mM), at room temperature (25 °C). (0 —, 4 —, 8 - - - - , 12 - - - - , 16 - - - - , 20 —, 40 - - - - , 60 —, 80 —, 100 —, 120 - - - - , 140 - - - - , 160 - - - - , 200 —, EtBr ~~~~~). Fluorescence emission changes against compound concentrations are also shown, (B) **12b**, (D) **13b**, (F) **12f**, (H) **13f**, (J) **12d**, (L) **13d**.

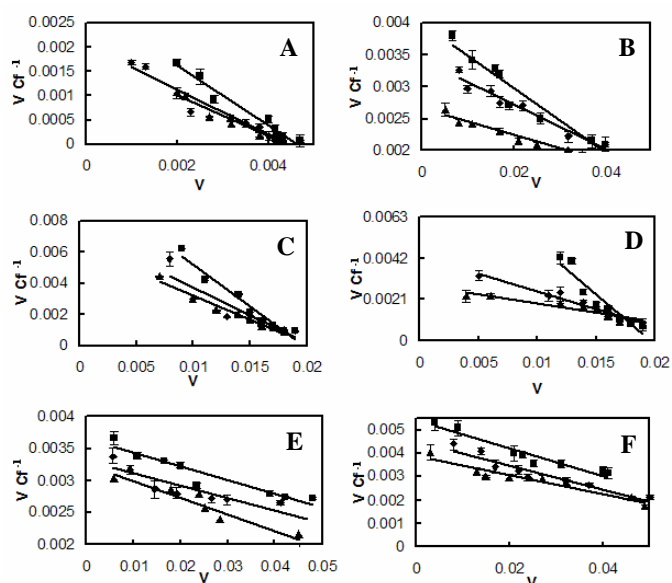


**Fig. 4.** Scatchard plots of compounds in Tris-HCl buffer (5 mM) at pH = 7.4, (A) **12b**, (B) **13b**, (C) **12f**, (D) **13f**, (E) **12d**, and (F) **13d** at concentrations of 50  $\mu\text{M}$  (■), 100  $\mu\text{M}$  (▲), and 150  $\mu\text{M}$  (●).

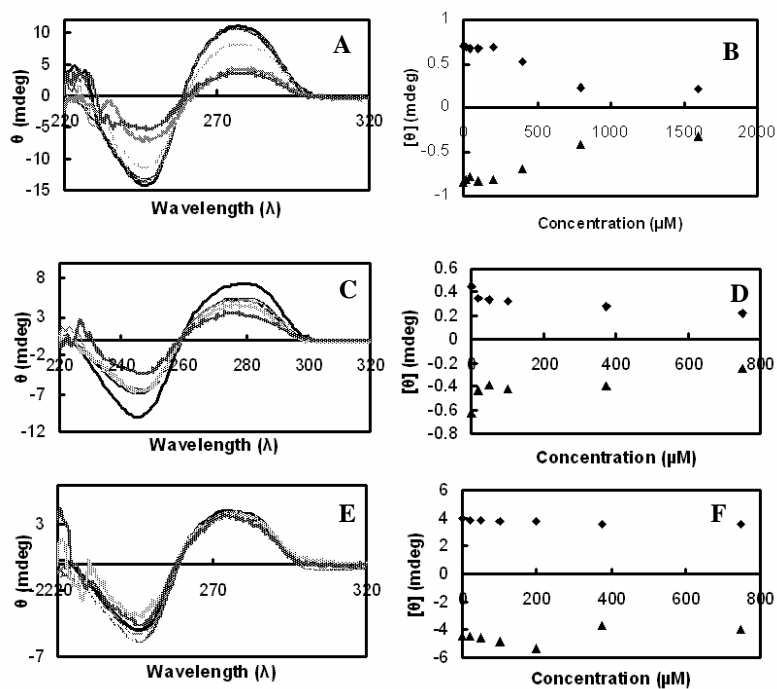


**Fig. 5.** CD absorption spectra of DNA in the absence and presence of ligands at different DNA to ligand concentration ratios of 0.04, 0.1, 0.2, 0.75, and 1.5 in each case. (A) **12b** (DNA —, 20 — —, 50 - - - - - , 100 ······, 200 - - - - - , 400 ······, 800 ······, 1600 ······), (C) **13f** (DNA —, 20 — —, 50 - - - - - , 100 ······, 375 ······, 750 ······), and (E) **13d** (DNA —, 20 — —, 50 - - - - - , 100 ······, 200 - - - - - , 375 ······, 750 ······). Molar ellipticity changes against different DNA/ligand ratios at 242 nm (▲) and 273 nm (■). (B) **12b**, (D) **13f**, (F) **13d** are also shown.

the CD spectra, among all the studied compounds, **12b** and **13f** are strongly capable of induction of conformational changes resulting from the disturbance in base pair stacking and strand helicity by forming additional hydrogen bonds probably with the oxygen of cytosine and the nitrogen of the imidazole ring (in the case of **13f**) or by forming non-covalent bonds between the  $\text{-NH}_2$  moiety of the guanine base and the oxygen of the nitro group in case of **12b**. In the case of **13f**, the benzyl group seems to have a pronounced effect in the induction of the more exposed conformation of the imidazole ring with critical moieties of the base pairs such as guanine and cytosine.

### Docking Simulations

The twelve synthesized compounds were docked onto  $\text{d}(\text{CGATCG})_2$  oligonucleotide according to the docking protocol [32]. Results indicate that a probable mode of action of acridinedione derivatives as DNA binding agents is via intercalation of the acridinedione moiety between base pairs with the imidazole substituent binding to the outer surface of the DNA bio-molecule, although there are other possible orientations due to molecular minimum energy conditions. As it can be seen from the docking simulation results (Fig. 6), the compounds are theoretically capable of intercalating within DNA double helix in a mode comparable to the reference

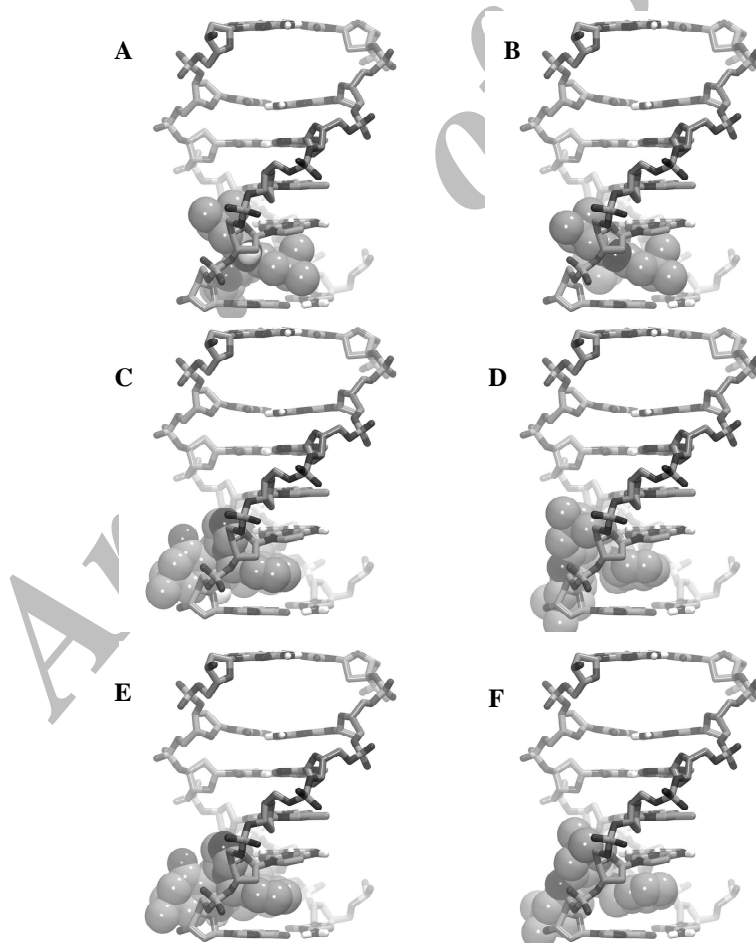


**Fig. 6.** Docking simulation results of (A) **12b**, (B) **13b**, (C) **12f**, (D) **13f**, (E) **12d**, (F) **13d**, with rendering in stick model for DNA bio-molecule and CPK for the compounds docked in DNA.

compound (Adriamycin). It is worth mentioning that apparently decreasing spatial hindrance in the area around the sliding moiety enhances the intercalating ability of the whole molecule.

### QSAR Analysis

The resulting correlation coefficient matrix is presented in

Table 3 for the selected descriptors. The numerical values of the descriptors selected by Eqs. (7-9) are listed in Table 4 and the brief description of these parameters is given in Table 5. The cross-validated prediction results and the predicted values are plotted against the experimental values.

Equation (7) is a monoparametric equation modeled for  $K_{app}$  of 11 compounds (compound **12a** was omitted as an

**Table 3.** Correlation Coefficient ( $R^2$ ) Matrix of the Selected Descriptors and Experimental Data Used in this Study

	ZM1V	Ram	PW3	MNC	$K_{app}$	$\Delta G$	$\log C_{50}$
ZM1V	1	0.763	0.038	-0.198	0.962	-0.486	-0.773
Ram		1	0.455	-0.021	0.779	-0.188	-0.884
PW3			1	0.200	-0.02	0.310	0.005
MNC				1	-0.18	0.782	0.252
$K_{app}$					1	-0.313	-0.871
$\Delta G$						1	0.389
$\log C_{50}$							1

**Table 4.** Numerical Values of the Calculated Descriptors Used in this Study

Compound	ZM1V	PJ13	MNC	Ram	PW3
<b>12a</b>	320	0.694	-0.3773	12	0.342
<b>13a</b>	336	0.735	-0.3407	12	0.342
<b>12b</b>	434	0.686	-0.3993	15	0.351
<b>13b</b>	450	0.785	-0.3746	15	0.351
<b>12c</b>	335.21	0.628	-0.3813	14	0.347
<b>13c</b>	351.21	0.821	-0.3406	14	0.347
<b>12d</b>	330	0.862	-0.3866	13	0.347
<b>13d</b>	346	0.741	-0.3421	13	0.347
<b>12e</b>	338.44	0.705	-0.068	14	0.355
<b>13e</b>	354.44	0.94	-0.4927	14	0.355
<b>12f</b>	394	0.872	-0.3968	14	0.339
<b>13f</b>	410	0.75	-0.3413	14	0.339

**Table 5.** Brief Description of Parameters Selected in the Study

Descriptors	Brief description
ZM1V	First Zagreb index by valence vertex degree
PJ13	3D Petijean Shape index
MNC	Most negative charge
Ram	Ramification index
PW3	Path/Walk 3- Randic shape index

outlier while deriving the corresponding model). The single topological descriptor, ZM1V explains 91.1% variance in  $K_{app}$ .

$$K_{app} = 0.001 (\pm 0.001) ZM1V - 0.260 (\pm 0.035)$$

$$(N = 11, R^2 = 0.911, Q^2 = 0.892, SE = 0.013, RMS = 0.013, F = 92.587, p = 0.001) \quad (7)$$

As can be seen, Eq. (8) has an acceptable quality and the variables used in this equation can explain 82.5% of variance in the interaction energy ( $\Delta G^o_{(H_2O)}$ ) of these derivatives. This model explains the positive effects of MNC and PJI3 on the interaction energy of the compounds. The positive sign of the coefficient of the MNC implies that the decrease in the negative charge of the molecule resulted in the enhanced interaction of the ligand and DNA. Because of the presence of negative charge on the outer surface of DNA macromolecule, increasing the MNC of the ligand resulted in the enhanced repulsive forces and therefore reduced interaction with DNA.

$$\Delta G^o_{(H_2O)} = 32.994 (\pm 5.147) MNC + 21.096 (\pm 5.639) PJI3 + 5.777 (\pm 3.973)$$

$$(N = 12, R^2 = 0.825, Q^2 = 0.721, SE = 1.543, RMS = 0.945, F = 21.274, p = 0.001) \quad (8)$$

Equation (9) explains 91.6% variance in the intercalation ability with respect to topological fields while LOO cross-validation power of prediction was found to be 84.2%. The model is dominated by the Ram descriptor with a negative coefficient. The second descriptor obtained in the equation is also the topological descriptor PW3 (positive coefficient).

$$\log C_{50} = -0.277 (\pm 0.030) Ram + 16.488 (\pm 4.652) PW3 - 0.342 (\pm 1.509)$$

$$(N = 11, R^2 = 0.916, Q^2 = 0.842, SE = 0.081, RMS = 0.045, F = 43.471, p = 0.001) \quad (9)$$

According to the models calculated above, the relatively higher affinities of the compounds **12b** and **13b**, can be explained thus: incorporating an electron withdrawing substituent on the 1,8-acridinedione moiety may decrease the electron density on the whole system especially the nitrogen atom of the pyridine or dihydropyridine ring, and make it more susceptible to gain positive charge, which enhances its attraction by negatively charged DNA molecules. The effect

of topological descriptors on the binding affinities did agree with the previous reports as well as with our predictions and expectations.

## CONCLUSIONS

The results of our investigations clearly show that all the synthesized ligands, differing only by the substituents of the imidazole ring, exhibit distinct DNA binding properties. Furthermore, it can simply be concluded from our diverse theoretical and experimental studies that there is no significant difference between the non-aromatic and aromatic derivatives. In sharp contrast with others, ligands **12b**, **13b**, **12f** and **13f** (bearing N-nitro and N-benzyl imidazole substituents) behave as typical non-competitive DNA intercalating agents, and their reasonably well binding to the double-stranded DNA provides a new template for DNA duplex stacking molecules. A few similar compounds containing the 1,8-acridinedione scaffold have been investigated for their mode of interaction with DNA, mostly showing non-intercalative (groove binding) behavior [40]. Finally, decreasing the electron density on the imidazole ring by the introduction of an electron-withdrawing substituent (*i.e.* nitro group) or a spatially flexible planar group (*i.e.* benzyl), diminishing the spatial hindrance of the tricyclic acridinedione moiety and ultimately, increasing the flexibility of the alkyl side chains attached to the central 1,8-acridinedione chromophore, are highly suggested for further modifications on similar DNA binding analogues. In addition, the presence of a nitro group can potentially have the extra advantage of increasing the selectivity of the new agent towards hypoxic cancer cells.

## ACKNOWLEDGEMENTS

This research was supported by Tehran University of Medical Science (TUMS), the University of Tehran (UT) and Iran National Science Foundation (INSF). Careful English editing of the manuscript by Dr. Nathaniel Martin is kindly acknowledged.

## REFERENCES

- [1] S. Catoen-Chackal, M. Facompre, R. Houssin, N. Pommery, J.F. Goossens, P.C. Bailly, J.P. He´nichart, J.

- Med. Chem. 47 (2004) 3665.
- [2] R. Martinez, L. Chacon-Garcia, *Current Med. Chem.* 12 (2005) 127.
- [3] A.A. Adjei, *Invest. New Drugs.* 17 (1999) 43.
- [4] J. Konopa, *Pure Appl. Chem.* 73 (2001) 1421.
- [5] J. Mazerski, K. Muchewicz, *Acta Biochimica Polonica* 47 (2000) 65.
- [6] P. Belmont, I. Dorange, *Expert Opin. Ther. Patents* 18 (2008) 1211.
- [7] K. Palani, P. Ambalavanan, M.N. Ponnuswamy, P. Murugan, V.T. Ramakrishnan, *Cryst. Res.* 40 (2005) 277.
- [8] S.J. Tu Qian Wang, J.P. Zhang, X.T. Zhu, J.N. Xu, *Acta Cryst. E61* (2005) 3743.
- [9] J. Jeyakanthan, M. Yogavel, T. Joseph Rajan, D. Velmurugan, K. Sekar, *Cryst. Res. Technol.* 37 (2002) 1029.
- [10] G. Murali, T.R. Miller, S.A. Buckner, I. Milicic, E.J. Molinari, L.K. Whitecker, R. Davis-Taber, V. E. Scott, C. Cassidy, J.P. Sullivan, W.A. Carroll, *Brit. J. Pharmacol.* 138 (2003) 393.
- [11] M.G. Gunduz, A.E. Dogan, R. Simsek, K. Erol, C. Safak, *Med. Chem. Res.* 18 (2009) 317.
- [12] S.A. Pandi, D. Velmurugan, M.M. Govind, M.J. Kim, T. Josephrajan, *Cryst. Res. Technol.* 37 (2002) 293.
- [13] K. Palani, D. Thirumalai, P. Ambalavanan, M.N. Ponnuswamy, V.T. Ramakrishnan, *J. Chem. Cryst.* 35 (2005) 751.
- [14] P. Murugan, K.C. Hwang, V.T. Ramakrishnan, S. Balasubramanian, *J. Materials Online* 1 (2005) 1.
- [15] W.D. McFadyen, N. Sotirellis, W.A. Denny, P.G. Wakelin, *Biochem. Biophys. Acta* 1084 (1990) 50.
- [16] A. Jamalian, R. Miri, O. Firuzi, M. Amini, A.A. Moosavi Movahedi, A. Shafiee, *J. Iran. Chem. Soc.* 8 (2011) 983.
- [17] S.Z. Bathaie, A.A. Moosavi-Movahedi, A.A. Saboury, *Nucleic Acids Res.* 27 (1999) 1001.
- [18] A.A. Saboury, *J. Iran. Chem. Soc.* 3 (2006) 1.
- [19] A.A. Saboury, A.A. Moosavi-Movahedi, H. Mansouri-Torshizi, *J. Chin. Chem. Soc.* 46 (1999) 917.
- [20] R.F. Greene, C.N. Pace, *J. Biol. Chem.* 249 (1974) 5388.
- [21] K.G. Strothkamp, R.E. Strothkamp, *J. Chem. Edu.* 71 (1994) 77.
- [22] A.J. Geall, I.S. Blagbrough, *J. Pharmaceut. Biomed. Anal.* 22 (2000) 849.
- [23] M. Howe-Grant, K.C. Wu, W.R. Bauet, S. Lippard, *J. Biochem.* 17 (1976) 1251.
- [24] H. Mansouri-Torshizi, M. Moghaddam, A. Divsalar, A.A. Saboury, *Bioorg. Med. Chem.* 16 (2008) 9616.
- [25] L. Fenghua, Z. Guanghua, W. Hongxing, Z. Shourong, L. Huakuan, *Trans. Metal Chem.* 31 (2006) 630
- [26] Y. Li, Z. Yang, T. Li, Z. Liu, B. Wang, *J. Fluoresc* 20 (2010) 891.
- [27] A.G. Krishna, D.V. Kumar, B.M. Khan, S.K. Rawal, K.N. Ganesh, *Biochim. Biophys. Acta* 1381 (1998) 104.
- [28] L. Peres-Flores, A.J. Ruiz-Chica, J.G. Delcros, F.M. Sanches, F.J. Ramirez, *Spectrochim. Acta Part A* 69 (2008) 1089.
- [29] M. Islami-Moghaddam, H. Mansouri-Torshizia, A. Divsalarb, A.A. Saboury, *J. Iran. Chem. Soc.* 6 (2009) 552.
- [30] G.M. Morris, D.S. Goodsell, R.S. Halliday, R. Huey, W.E. Hart, R.K. Belew, A.J. Olson, *J. Comput. Chem.* 19 (1998) 1639.
- [31] L.D. Frederick, G. Williams, G.A. Ughetto, J.H. Van der Marel, R. Van Boom, H.J. Wang, *Biochemistry* 29 (1990) 2538.
- [32] A. Madadkar-Sobhani, S. Rasoul amini, J.D.A. Tyndall, E. Azizi, M. Daneshtalab, A. Khalaj, *J. Mol. Graph. Model.* 25 (2006) 459.
- [33] M.J. Frisch, M.J. Trucks, H.B. Schlegel, G.E. Scuseria, M.A. Robb, J.R. Cheeseman, V.G. Zakrzewski, J.A. Montgomery, J.R. Stratmann, J.C. Burant, S. Dapprich, J.M. Millam, A.D. Daniels, K.N. Kudin, M.C. Strain, O. Farkas, J. Tomasi, V. Barone, M. Cossi, R. Cammi, B. Mennucci, C. Pomelli, C. Adamo, S. Clifford, J. Ochterski, G.A. Petersson, P.Y. Ayala, Q. Cui, K. Morokuma, D.K. Malick, A.D. Rabuck, K. Raghavachari, J.B. Foresman, J. Cioslowski, J.V. Ortiz, A.G. Baboul, B.B. Stefanov, G. Liu, A. Liashenko, P. Piskorz, I. Komaromi, R. Gomperts, R.L. Martin, D.J. Fox, T. Keith, M.A. Al-Laham, C.Y. Peng, A. Nanayakkara, C. Gonzalez, M. Challacombe, P.M.W. Gill, B. Johnson, W. Chen, M.W. Wong, J.L. Andres, C. Gonzalez, M. Head-Gordon, E.S. Replogle, J.A. Pople, *Gaussian 98, Revision A.7, Pittsburgh PA Inc.,*

Novel Imidazolyl Derivatives of 1,8-Acridinedione as Potential DNA-Intercalating Agents

- Pennsylvania, 1998.
- [34] M. Khoshneviszadeh, N. Edraki, R. Miri, B. Hemmateenejad, *Chem. Biol. Drug Des.* 72 (2008) 564.
- [35] R. Miri, K. Javidnia, H. Mirkhani, B. Hemmateenejad, Z. Sepehr, M. Zalpour, T. Behzad, M. Khoshneviszadeh, N.A.R. Edraki, Mehdipour, *Chem. Biol. Drug Des.* 70 (2007) 329.
- [36] N. Edraki, B. Hemmateenejad, R. Miri, M. Khoshneviszadeh, *Chem. Biol. Drug Des.* 70 (2007) 530.
- [37] A.A. Moosavi Movahedi, B. Samiee, G.H. Hakimelahi, *J. Colloid Interface Sci.* 161 (1993) 53.
- [38] C.N. Pace, *TIB Tech.* 8 (1990) 93.
- [39] R.J. Fiel, *J. Biol. Struct. Dyn.* 6 (1989) 1259.
- [40] A. Rajendran, B. Unni Nair, *Biochim. Biophys. Acta* 1760 (2006) 1794.

Archive of SID